Communications on Applied Nonlinear Analysis
ISSN: 1074-133X
Vol 31 No. 7s (2024)

Heat Transfer Analysis of Bingham Fluid Flow in the Entrance Region of Concentric Annuli with Outer Cylinder Rotating

Gayathri devi Nangineni[1], N. Sinivasa Rao[2*] and M. Venkata Subba Rao[3]

[1] Research Scholar, Department of Mathematics and Statistics, School of Applied Science and Humanities, Vignan's Foundation for Science, Technology and Research, Vadlamudi, Andhra Pradesh - 522 213, India

[1]Email: ngayathridevi55@gmail.com

[2]Division of Mathematics, Department of Basic Science and Humanities, GMR Institute of Technology, Rajam, Vizianagaram, A.P, India - 532127

[2]Email: srinivasarao.n@gmrit.edu.in

[2]Department of Mathematics and Statistics, School of Applied Science and Humanities, Vignan's Foundation for Science, Technology and Research, Vadlamudi, Andhra Pradesh - 522 213, India

[3]Email: mail2mvsr@gmail.com

Article History:

Received: *01-06-2024*

Revised: *03-07-2024*

Accepted: *29-07-2024*

Abstract:

The aim of this study is to analyze the heat transfer characteristics of Bingham fluid flow in the entrance region of concentric annuli, where the inner cylinder remains stationary and the outer cylinder is in rotation. This rotational motion of the outer cylinder induces the flow within the annular region. The governing equations for this flow are solved using a robust numerical technique known as the finite difference method. This investigation focuses on the transient expansion of thermal and hydrodynamic boundary layers within the concentric annuli, considering different boundary conditions: one section being isothermal while another is adiabatic. The outer cylinder is assumed to rotate at a constant angular velocity, while the inner cylinder is kept stationary. A finite difference analysis is employed to obtain velocity distributions, pressure drops, and temperature variations along the radial direction. Some of the observations are increase in the aspect ratio (M) leads to a corresponding rise in axial velocity for all examined Bingham number (B) variations and temperature is seen to rise as the Bingham numeral B and aspect ratio M increases. This comparative analysis helps validate the current investigation's results and confirms their accuracy and reliability.

Keywords: Bingham fluid, Entrance region, Concentric annulus, Finite difference method, Rotating cylinder.

Nomenclature:

M	Aspect ratio of the annulus
u, v, and w	Velocity components in z, r, θ directions, respectively
u_0	Uniform inlet velocity
U, V, W	Dimensionless velocity components
p	Pressure
p_0	Initial pressure
P	Dimensionless pressure
r, θ and z	cylindrical coordinates
R, Z	Dimensionless coordinates in the radial and axial directions, respectively

R_1, R_2	Radius of the inner and outer cylinders, respectively
B	Bingham number
Re, Ta	Modified Reynolds number and Taylor number respectively
ρ	Density of the fluid
μ	Apparent viscosity of the model
τ	Shear stress
τ_0	Bingham yield Stress
ω	Regular angular velocity
Pr	Prandtl number
R, Z	Mesh sizes in the radial and axial directions, respectively.

1. INTRODUCTION:

Engineering applications such as the design of compact heat exchangers, axial-flow turbo devices, and polymer processing highlight the relevance of studying heat transfer in the thermal entrance zone of annuli with non-Newtonian laminar flow. Laminar flow operations are preferable in a variety of situations, including maintaining a low pumping power to heat transfer rate ratio. In sectors such as nuclear reactors, where heating begins at the duct entry, the hydrodynamic boundary layers are linear near the entrance and shift to turbulence downstream. As a result, it is critical to evaluate the presence of laminar entry flow while analysing heat transfer characteristics in ducts with turbulent fully developed flow.

Many significant industrial fluids exhibit rheological properties, characterized by non-Newtonian flow behavior. Examples include paints, glues, inks, foods, diverse suspensions like coal water or coal-oil slurries, and biological fluids like blood. The fluid, categorized as Bingham, is classified as a "time-independent yield stress" fluid.

Coney and El-Shaarawi [1] investigated the predicament of Newtonian fluid foyer constituency stream and temperatures transmit in a concentric annulus. Mishra et al [2] got the consequences for periphery stratum width, centre nucleus haste, and stress slump by analysing the stream of Bingham synthetic liquefied in the concentric annulus. Batra and BigyaniDas [3] the internal container is at respite and the external container is revolving while the stress-strain relation intended for Casson liquefied within the annular gap flanked by two coaxial gyratory containers is created. Gasparetto and Maia [4] Applying the limited dissimilarity approach to the Power-law liquefied in the annuli, different entrance geometries were discovered. Hazem and Sayed-Ahmed [5] employed the restricted differentiation approach to analyse laminar Power-Law fluid stream in a rotatable inner wall, concentric annulus.

The constitutive equalization for Bingham liquefied is specified as Bird et al [6]

$$\tau_{ij} = \left(\mu + \frac{\tau_0}{\varepsilon}\right)\varepsilon_{ij} \quad (\tau > \tau_0) \tag{1}$$

Where

$$\tau = \sqrt{\frac{1}{2}\tau_{ij}\tau_{ij}} \qquad and \qquad \varepsilon = \sqrt{\frac{1}{2}\varepsilon_{ij}\varepsilon_{ij}}$$

here τ_{ij}, and $\varepsilon_{ij}$are the strain tensor and the tempo of sprain tensor correspondingly and τ_0 is the yield stress and liquefied velocity is μ.

Kandasamy [7] investigated the velocity profiles, temperature distribution, and pressure characteristics within the entrance region of flow in concentric annuli for a Bingham fluid. Galanis and Rashidi [8] examined the entropy generation in Non-Newtonian fluids, focusing on heat and mass transfer in the entrance region of channels. This work built on the earlier research by Round and Yu [9], who had explored the developing flows of Herschel-Bulkley fluids in concentric annuli. More recently, Kandasamy and Srinivasrao [10] conducted a study on the heat transfer characteristics of the flow in the entrance region, with a rotating inner wall, for Bingham fluids within concentric annuli. Zadorozhnyi [11] conducted a study aimed at determining the productivity (Q), which represents the relative flow rate, and the speed of the central core ($\Delta U\rho$), based on various parameters of the concrete mixture and the radius of the pipeline (R).

Mullai Venthan and Jayakaran Amalraj [12] conducted an in-depth investigation into the flow characteristics of a non-Newtonian fluid within the entrance region of the annular space between two coaxial cylinders in rotation. This fluid is time-independent and follows Bingham's stress–strain relations. Chithrakumar et al. [13] explored the experimental aspects of convective heat transfer from an inner stationary heated cylinder located within a vertical concentric annulus, where the outer cylinder is in rotation. Their research focused on understanding the heat transfer dynamics in this specific configuration.

Arain et al. [14] investigated the flow characteristics of a non-Newtonian Sutterby fluid containing tiny particles and the resulting magnetic field, also accounting for the presence of motile gyrotactic microorganisms. Bhatti et al. [15] developed a mathematical model to simulate steady, laminar, exothermic reactive electromagneto-hydrodynamic transport of a combustible non-Newtonian fluid in a vertical duct under natural convection conditions. Additionally, Pratik Anhor and Mohammad Atif [16] considered a Taylor-Couette setup with radial heating, where a Boussinesq fluid undergoes shear within the annular region formed between two concentric cylinders that rotate independently and are maintained at different temperatures.

Hari Babu et al. [17] conducted a study on the unsteady MHD convective flow of Casson hybrid nanofluid over permeable media with ramped wall temperature, presenting several notable observations. One of their key findings was that the resulting velocity increased with the enhancement of heat and concentration buoyancy strengths, while the slip parameter had the opposite effect in the case of ramped wall temperatures. Additionally, Hari Babu et al. [18] provided detailed observations on heat and mass transfer in unsteady MHD Casson fluid flow past an infinite vertical porous plate with chemical reactions. Babu BH et al. [19] studied the numerical modeling of activation energy and hydromagnetic non-Newtonian fluid particle deposition flow on a rotating disc. Furthermore, Hari Babu et al. [20] investigated the hall and ion-slip effects on MHD free convection flow of rotating Jeffrey fluid over an infinite vertical porous surface. Lastly, Hari Babu et al. [21] examined the non-linear radiation and dissipative impacts on non-Newtonian hydromagnetic Falkner-Skan fluid through a wedge

The flow and heat transfer properties of Bingham fluid at the entrance region of concentric annuli were examined in this work. In our study, the inner cylinder is considered to be fixed while the outer cylinder rotates. We used a linear explicit finite difference approach to discretize and solve the conservation equations for mass, momentum, and energy using Prandtl's boundary layer assumptions. The Gauss-Jordan technique was used to successfully solve the resultant system of linear algebraic equations. We discovered the development of the temperature distribution at the entry region by examining a variety of non-Newtonian flow behaviours and geometric factors. We also explore the effects of these variables on pressure distribution and velocity profiles.

2. MATHEMATICAL FORMULATION:

Diagram 1 depicts the calculation of the issue. The Bingham liquefied pierce the parallel concentric annuli through internal and external radii of R_1 & R_2, correspondingly, commencing a huge compartment with a homogeneous horizontal swiftness silhouette u_0 beside the axial track z and through a preliminary heaviness p_0 and warmth t_0. While the outer cylinder swivels at a raw-boned swiftness, the internal container is at respite. The flow is stable, laminar, incompressible, and axisymmetric, with low viscosity and no internal heat generation, and these physical features are constant. Axial heat diffusion is also likely to be negligible in comparison to radial diffusion. This research considers a cylinder-shaped polar coordinate system with the radial track r running vertical to annulus's central axis, origin at the inlet section, and the z-axis running equivalent to it.

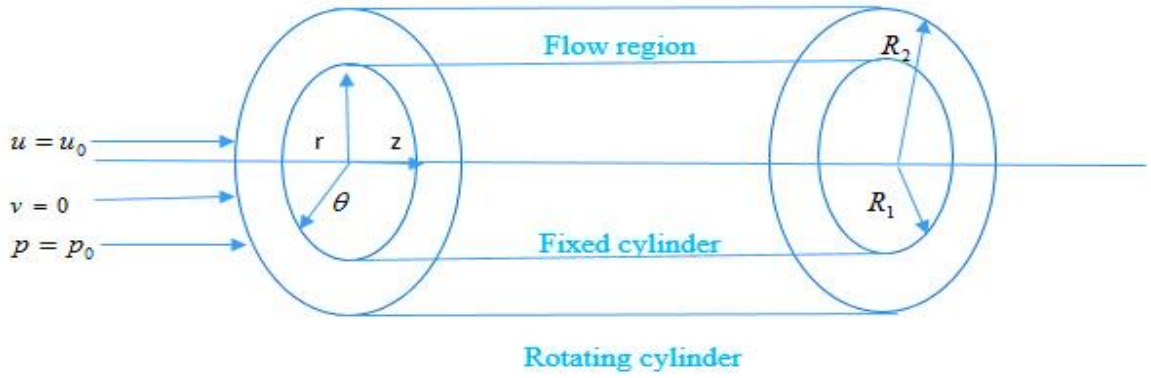

Figure 1. Flow Diagram

Using the aforementioned hypotheses along through the standard Prandtl's periphery stratum hypotheses [16], the prevailing calculations for a Bingham liquefied in the foyer area in polar coordinates r, θ, z are:

Continuity equation: $\frac{\partial(rv)}{\partial r} + \frac{\partial(ru)}{\partial z} = 0$ (2)

r-momentum equation: $\frac{\omega^2}{r} = \frac{1}{\rho}\frac{\partial p}{\partial r}$ (3)

θ-momentum equation :$v\frac{\partial w}{\partial r} + u\frac{\partial w}{\partial z} + \frac{vw}{r} = \frac{1}{\rho r^2}\frac{\partial}{\partial r}(r^2\left[\tau_0 + \mu r\frac{\partial}{\partial r}\left(\frac{w}{r}\right)\right])$ (4)

z-momentum equation : $v\frac{\partial u}{\partial r}+u\frac{\partial u}{\partial z}=-\frac{1}{\rho}\frac{\partial p}{\partial z}+\frac{1}{\rho}\frac{\partial}{\partial r}(r[\tau_0+\mu\frac{\partial u}{\partial r}])$ (5)

Energy equation :$v\frac{\partial t}{\partial r}+u\frac{\partial t}{\partial z}=\alpha[\frac{\partial^2 t}{\partial r^2}+\frac{1}{r}\frac{\partial t}{\partial r}]$ (6)

Where u,v,w are swiftness mechanisms in the direction z,r,θ correspondingly, t is liquefied warmth at several tip,ρ is the concreteness of the liquefied, α is the tepid dissipation and p is the heaviness.

The boundary conditions for the present study are:

For $z\geq 0$and $r=R_1,\ v=u=w=0$

For $z\geq 0$and $r=R_2,\ v=u=0$ and $w=\omega R_2$

For $z=0$and $R_1<r<R_2$, $u=u_0$ at $z=0, p=p_0$ (7)

Using the periphery circumstances (7), the permanence calculation (2) can be articulated in the subsequent fundamental variety:

$2\int_{R_1}^{R_2} ru\,dr=(R_2^2-R_1^2)u_0$ (8)

Introducing the following dimensionless variables and parameters (see for example, Kandasamy and Srinivas Rao [10]):

$$R=\frac{r}{R_2},U=\frac{u}{u_0},V=\frac{\rho v R_2}{\mu_r},\ W=\frac{w}{\omega R_2},$$

$$M=\frac{R_1}{R_2},\ P=\frac{p-p_0}{\mu_r},Z=\frac{2z(1-M)}{R_2 Re},T=\frac{t-t_0}{t_w-t_0},B=\frac{\tau_0 R_2}{k u_0}$$

$$Re=\frac{2\rho(R_2-R_1)u_0}{k},\ \mu_r=\mu\left(\frac{\omega R_1}{R_2}\right),T_a=\frac{2\omega^2\rho^2 R_1^2(R_2-R_1)^3}{\mu_r^2(R_1+R_2)},Pr=\frac{\mu C_p}{K}$$

Here the Bingham numberis , the Reynolds number is Re, T_a is the Taylor number,Reference viscosity is known asμ_r,prandtl's number is known asPr,$C_p$is the unambiguous warmth at invariable temperature, K is the thermic dynamism and $M$is the aspect ratio of the annulus.

Equations (2) to (6) and (8) in the dimensionless variety are prearranged by

$\frac{\partial V}{\partial R}+\frac{V}{R}+\frac{\partial U}{\partial Z}=0$ (9)

$\frac{W^2}{R}=\frac{Re^2(1-M)}{2(1+M)T_a}\frac{\partial P}{\partial R}$ (10)

$V\frac{\partial W}{\partial R}+U\frac{\partial W}{\partial Z}+\frac{VW}{R}=\frac{\partial^2 W}{\partial R^2}+\frac{1}{R}\frac{\partial W}{\partial R}-\frac{W}{R^2}+\frac{2B}{R}$ (11)

$V\frac{\partial U}{\partial R}+U\frac{\partial U}{\partial Z}=-\frac{\partial P}{\partial Z}+\frac{1}{R}\frac{\partial U}{\partial R}+\frac{\partial^2 U}{\partial R^2}+\frac{B}{R}$ (12)

$V\frac{\partial T}{\partial R}+U\frac{\partial T}{\partial Z}=\frac{1}{Pr}[\frac{\partial^2 T}{\partial R^2}+\frac{1}{R}\frac{\partial T}{\partial R}]$ (13)

$2\int_M^1 RU\,dR=(1-M^2)$ (14)

The boundary conditions (7) in the dimensionless form are:

For $Z \geq 0$ and $R = M,\ V = U = W = 0$

For $Z \geq 0$ and $R = 1,\ V = U = 0$ and $W = 1$

For $Z = 0$ and $M < r < 1\ ,\ U = 1$ at $Z = 0, P = 0$ (15)

For the thermal analysis, we have considered the scenario where the outer cylinder is maintained at a constant temperature (isothermal) and the inner cylinder does not allow heat transfer (adiabatic). The solution to the problem has been derived under these specific boundary conditions.

For$Z \geq 0\ ,\ T = 1$ at $R = 1$

For $Z \geq 0\ ,\ \frac{\partial T}{\partial R} = 0$ at $R = M$ (16)

For $Z = 0$and $M < r < 1\ ,\ T = 0$

In a similar manner, the problem can be analyzed for the reverse scenario, where the inner cylinder is maintained at a constant temperature (isothermal) and the outer cylinder is adiabatic. The boundary conditions for this reversed scenario will be adjusted accordingly to reflect the isothermal nature of the inner cylinder and the adiabatic condition of the outer cylinder.

For $Z \geq 0\ ,\ T = 1$ at $R = M$

For $Z \geq 0\ ,\ \frac{\partial T}{\partial R} = 0$ at $R = 1$ (17)

For $Z = 0$and $M < r < 1\ ,\ T = 0$

3. NUMERICAL SOLUTION

The numerical analysis and solution methodology can be viewed as an indirect expansion of the research conducted by Kandasamy and Srinivas Rao [10]. The finite difference approach has an essential benefit in terms of simplicity. It also makes it simple to achieve high-order approximations, which allows for high-order precision in spatial discretization. However, the primary limitations include computational cost, complexity, considerable computer storage needs, and associated communication challenges. The following discrete representations are created using the mesh network shown in Fig. 19 In this context, ΔR and ΔZ denote the grid size along the radial and axial directions, respectively.

$$\boldsymbol{V_{i+1,j+1} = V_{i,j+1}\left(\frac{M+i\Delta R}{M+(i+1)\Delta R}\right) - \frac{\Delta R}{4\Delta Z}\left(\frac{2M+(2i+1)\Delta R}{M+(i+1)\Delta R}\right)\left(U_{i+1,j+1} + U_{i,j+1} - U_{i+1,j} - U_{i,j}\right)} \quad \textbf{(18)}$$

$$\frac{W_{i,j+1}^2}{M+i\Delta R} = \frac{(1-M)Re^2}{2T_a(1+M)}\frac{P_{i,j+1}-P_{i-1,j+1}}{\Delta R} \quad (19)$$

$$V_{i,j}\left[\frac{W_{i+1,j+1}+W_{i+1,j}-W_{i-1,j}-W_{i-1,j+1}}{4\Delta R}\right] + U_{i,j}\left[\frac{W_{i,j+1}-W_{i,j}}{\Delta Z}\right] + \frac{V_{i,j}W_{i,j}}{M+i\Delta R} =$$
$$\frac{W_{i+1,j+1}+W_{i+1,j}-2W_{i,j+1}-2W_{i,j}+W_{i-1,j}+W_{i-1,j+1}}{2(\Delta R)^2} + \frac{W_{i+1,j+1}+W_{i+1,j}-W_{i-1,j}-W_{i-1,j+1}}{(M+i\Delta R)4\Delta R} - \frac{W_{i,j}}{(M+i\Delta R)^2} + \frac{2B}{M+i\Delta R} \quad (20)$$

$$\boldsymbol{V_{i,j}\left[\frac{U_{i+1,j+1}-U_{i-1,j+1}}{2\Delta R}\right]+U_{i,j}\left[\frac{U_{i,j+1}-U_{i,j}}{\Delta Z}\right]=}$$

$$-\frac{P_{i,j+1}-P_{i,j}}{\Delta Z}+\frac{U_{i+1,j+1}-U_{i-1,j+1}}{(M+i\Delta R)2\Delta R}+\frac{U_{i+1,j+1}-2U_{i,j+1}+U_{i-1,j+1}}{(\Delta R)^2}+\frac{B}{M+i\Delta} \quad (21)$$

Where $\boldsymbol{i=0}$ at $\boldsymbol{R=1}$ and $\boldsymbol{i=m}$at $\boldsymbol{R=M}$, respectively

The result of applying the trapezoidal regulation to an calculation (2.11) is

$$\int_M^1 ru\,dr=\frac{\Delta R}{2}[Mu_0,j+1u_m,j]+\Delta R\sum_{i=1}^{n-1}u_{i,j}R_i$$

The boundary conditions (15) gives $\boldsymbol{u_0,j=u_m,j=0}$ and the above equations reduced to

$$\int_M^1 ru\,dr=\Delta R\ \sum_{i=1}^{m-1}u_{i,j}(M+i\,\Delta R)=\frac{1-M^2}{2} \quad (22)$$

Through an iterative process, the position of distinction calculations (18) to (22) has been unraveling. Pertain equation (20) for $\leq i\leq n-1$ and preliminary at the column j=0 article (annulus entry), we obtain a scheme of linear numerical equations.

The standards of the swiftness element W in the subsequent article with $j=1$. have been unwavering by resolving this predicament using the Gauss-Jordan scheme. The scheme of linear calculations is then acquired by via calculations (19) and (21) for $\leq i\leq n-1$and calculation (22). To acquire the standards of the swiftness element U and the heaviness P at the jiffy column $j=1.$, solve this problem again using the Gauss-Jordan scheme. Finally, given the known standards of U, the standards of the swiftness element Vin in the second column with $j=1$ are calculated using the Gauss-Jordan method from equation (18). By repeating this process, we can go along the annulus' axial track, discourse by discourse, until the stream is fully formed together axially and imaginatively.

The power calculation (13) can be viewed as a linear calculation in T with inconsistent coefficients once the standards of V and U are recognized. The power calculation can be expressed by the implicit finite difference method as

$$T_{i+1,j+1}\left(\frac{V_{i,j+1}+V_{i,j}}{8\Delta R}-\frac{1}{2\Pr(\Delta R)^2}-\frac{1}{4(M+i\Delta R)Pr\Delta R}\right)+T_{i,j+1}\left(\frac{U_{i,j+1}+U_{i,j}}{2\Delta Z}+\frac{1}{\Pr(\Delta R)^2}\right)$$

$$+T_{i-1,j+1}\left(\frac{1}{4(M+i\Delta R)Pr\Delta R}-\frac{V_{i,j+1}+V_{i,j}}{8\Delta R}-\frac{1}{2\Pr(\Delta R)^2}\right)$$

$$=T_{i,j}\left(\frac{U_{i,j+1}+U_{i,j}}{2\Delta Z}-\frac{1}{\Pr(\Delta R)^2}\right)+T_{i+1,j}\left(\frac{1}{2\Pr(\Delta R)^2}+\frac{1}{4(M+i\Delta R)Pr\Delta R}-\frac{V_{i,j+1}+V_{i,j}}{8\Delta R}\right)+T_{i-1,j}\left(\frac{V_{i,j+1}+V_{i,j}}{8\Delta R}+\right.$$

$$\left.\frac{1}{2\Pr(\Delta R)^2}+\frac{1}{4(M+i\Delta R)Pr\Delta R}\right)$$

The warmth profiles in the annular entry province have been obtained by solving Calculation (23), along with the periphery circumstances (16). The Gauss-Jordan elimination scheme has been used to resolve the scheme of linear calculations related to each column.

Table 1: Comparison of non-Newtonian fluids in particular cases with the Newtonian fluids

Fluid	When yield stress τ_0	When flow index n	Becomes
Bingham Model	0	Not applicable	Newtonian fluid
Herschel-Bulkley fluid	0	1	Newtonian fluid
Power -law Model	Not applicable	1	Newtonian fluid

We conducted a comparison between the Bingham model results and the cases discussed earlier. Our analysis revealed that the results from the Bingham model closely aligned with those obtained for Newtonian fluids.

4. RESULTS AND DISCUSSION.

All possible values of the Bingham number (B) and aspect ratio (M) have been calculated numerically, and 14 has been selected as Prandtl's number. For M=0.4 and 0.9, respectively, the Reynolds number to Taylor number ratio, $Rt = \frac{Re^2}{T_a}$ has been adjusted to 20, 10, with ΔZ values of 0.01 and 0.02, and ΔR values of 0.1 and 0.05, for M=0.4 and 0.9, respectively. For M=0.4, 0.9, and B=0, 5, 10, 15 the radial temperature distribution, velocity and pressure distribution profiles have been calculated. The radial temperature distribution has been plotted for various axial positions with M=0.4, 0.9, B=0, 5, 10, 15, and Pr=14. There has been much discussion of the effects of geometric factors and non-Newtonian properties on velocity profiles and pressure drop elsewhere. The temperature distributions during the rotation of the outer wall of the annuli are illustrated in the following Figs. 3 to 10. The data shows that for a given annular width, the temperature increases as the Bingham number grows, likely due to increased viscous dissipation in the fluid. Conversely, for a constant Bingham number, the temperature decreases as the aspect ratio increases, possibly because a larger aspect ratio allows for better heat dissipation. Additionally, it is found that with a fixed aspect ratio M, Bingham number B, and Prandtl number, the temperature rises with an increase in axial position, which could be attributed to the accumulation of thermal energy along the axial direction.

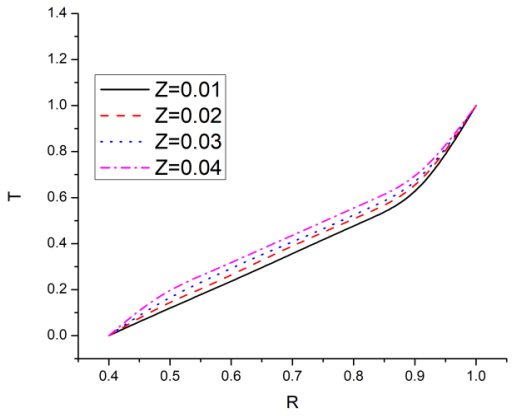

Fig .3: Temperature profile for M=0.4, Pr=14, B=0

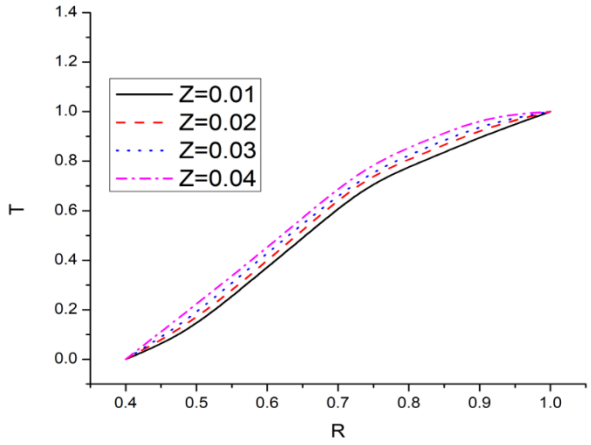

Fig .4: Temperature profile for M=0.4, Pr=14, B=5

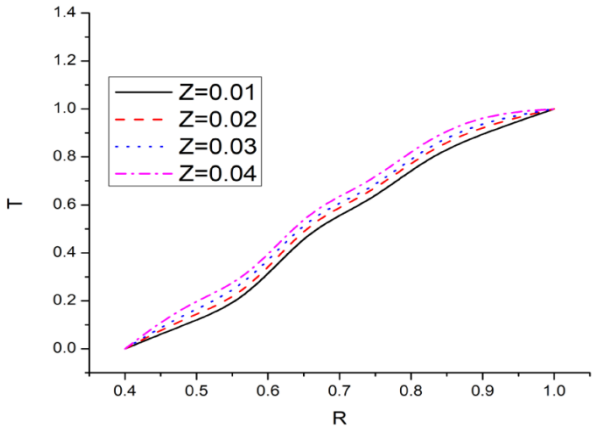

Fig .5: Temperature profile for M=0.4, Pr=14, B=10

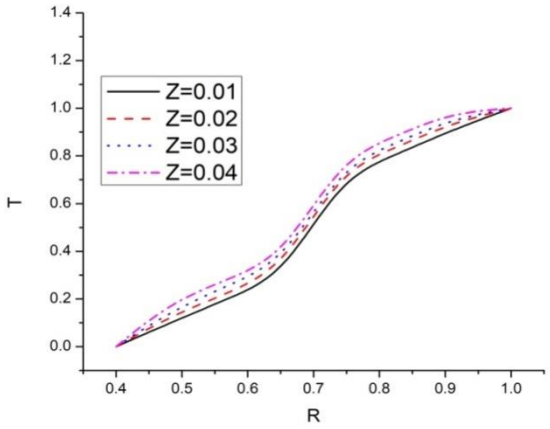

Fig .6: Temperature profile for M=0.4, Pr=14, B=15

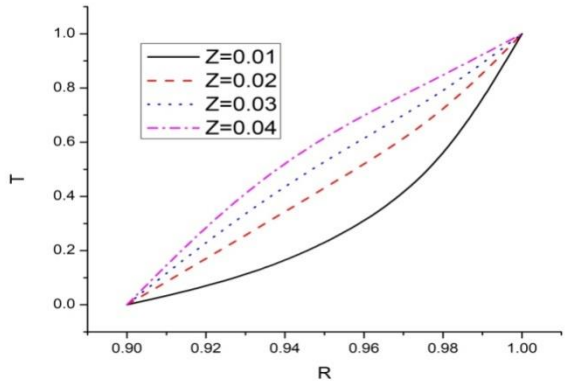

Fig .7: Temperature profile for M=0.9, Pr=14, B=0

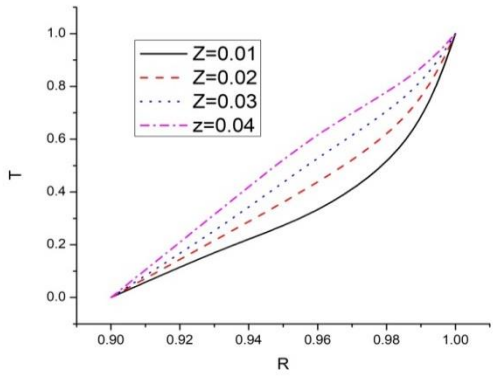

Fig .8: Temperature profile for M=0.9, Pr=14, B=5

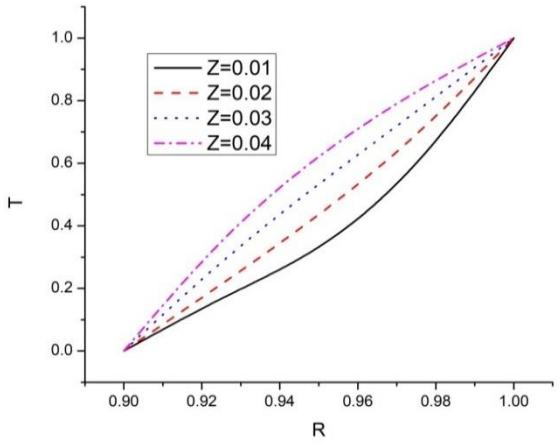

Fig .9: Temperature profile for M=0.9, Pr=14, B=10

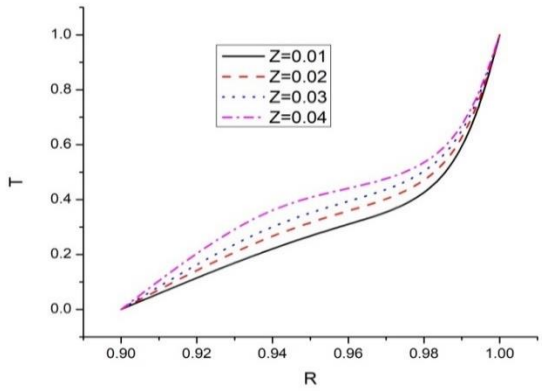

Fig .10: Temperature profile for M=0.9, Pr=14, B=15

Figs. 11 to 12 depict the tangential velocity profile growth for aspect ratio (M) of 0.2 and 0.7 at various axial locations (Z = 0.03) across different Bingham numbers (B), with Rt set to 20. Tangential velocity increases within the annulus from the inner cylinder wall to the outer cylinder wall. The profile expands with an increase in aspect ratio, indicating higher velocity for shorter annuli spacing. Additionally, higher Bingham numbers correspond to increased tangential velocity for rotating outer cylinders. The impact of parameter Rt on tangential velocity is minimal, as shown in various Rt values.

Figs. 13 to 14 illustrate the axial velocity profile component (U) evolution for M = 0.2 and 0.7 at Z = 0.03, considering different Bingham numbers. Calculations span various Rt values, with results displayed for Rt = 20. Component velocity U grows with both Bingham value (B) and aspect ratio (S). A parabolic shape is observed in the velocity profile when Bingham number B is zero, for both stationary (Rt = 0) and spinning (Rt = 20) outer cylinders. Rotation's impact on axial velocity is relatively minimal, consistent with previous studies.

Figs. 15 to 16 present the radial velocity profile (V) for M = 0.2 and 0.7 at Z = 0.03, considering various Bingham and Rt values. Radial velocity values are negative near the inner cylinder wall because it moves in the opposite direction as the radial coordinate, but positive near the outer cylinder wall because it moves in the same direction as the radial coordinate. At any axis cross section, the radial velocity values drop as Rt and Bingham number grow. The results of certain situations, such as Rt=0 and B=0, are totally compatible with previous investigations [7].

Figs. 17 to 18 demonstrate the pressure distribution along the radial coordinate for the same values. Pressure rises from the inner wall's maximum to the outer wall's minimum; greater Bingham values indicate higher pressure. Reason behind this that thick, viscous fluid generally exhibit higher pressures. Additionally, the pressure becomes relatively independent of the radial coordinate near the inner wall. Across any cross-section, the rotation of the outer cylinder has minimal impact on fluid pressure.

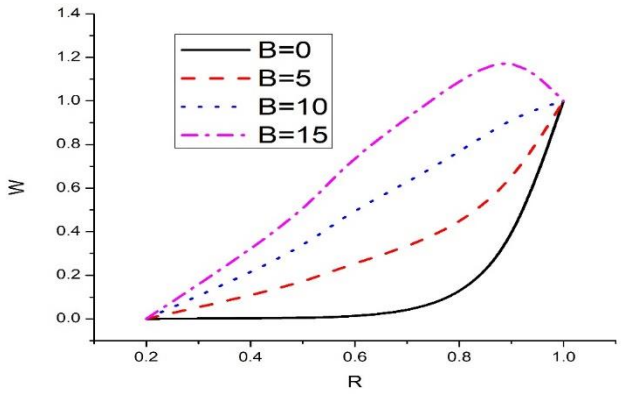

Fig. 11: Tangential velocity profile for M = 0.2 at Z = 0.03

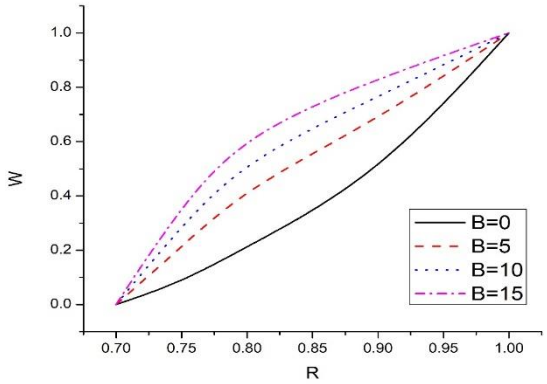

Fig. 12: Tangential velocity profile for M = 0.7 at Z = 0.03

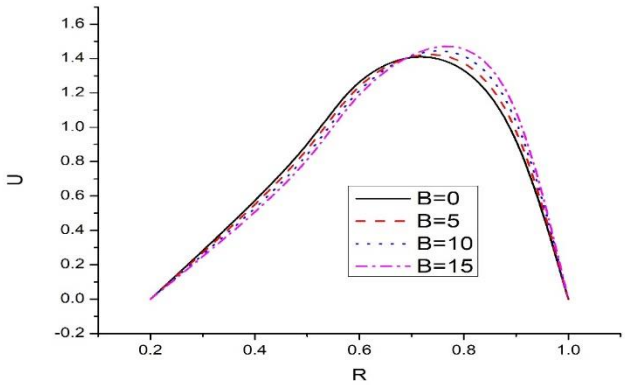

Fig. 13: Axial velocity profile for M = 0.2 at Z = 0.03

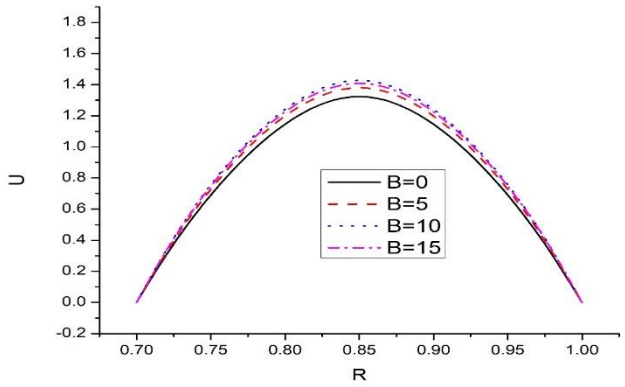

Fig. 14: Axial velocity profile for M = 0.7 at Z = 0.03

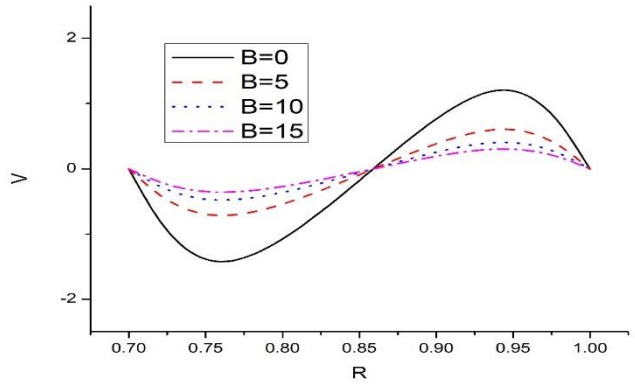

Fig. 15: Radial velocity profile for M = 0.2 at Z = 0.03

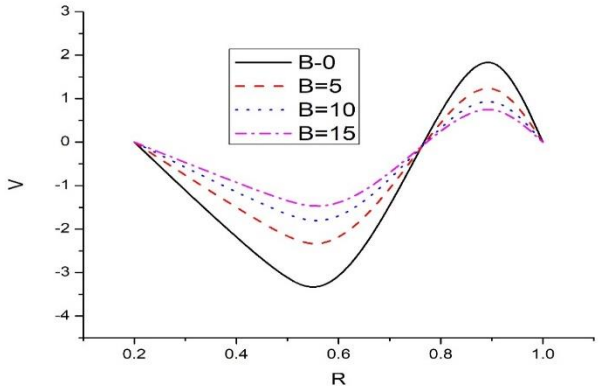

Fig. 16: Radial velocity profile for M = 0.7 at Z = 0.03

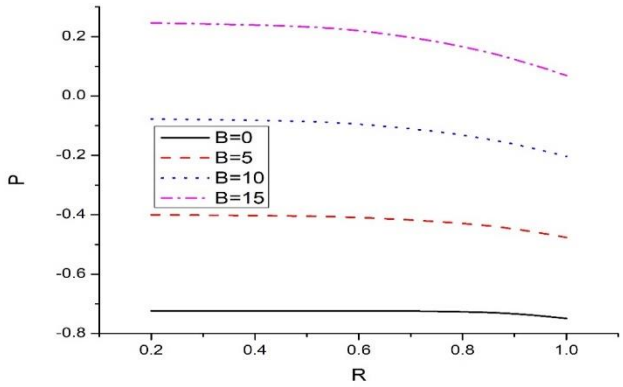

Fig. 17: Pressure distribution for M = 0.2 at Z = 0.03

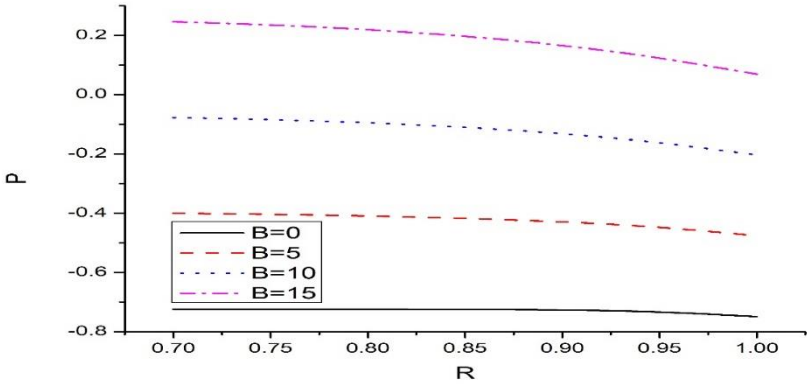

Fig. 18: Pressure distribution for M = 0.7 at Z = 0.03

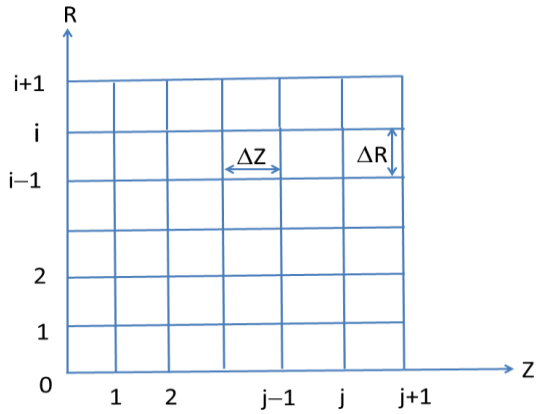

Fig. 19: Grid configuration for Finite-Difference demonstrations.

5. CONCLUSIONS

The paper presents numerical findings concerning heat transfer within the entry region of concentric annuli featuring rotating outer walls, focusing particularly on Bingham fluids. It explores how various factors, such as aspect ratio (M), Bingham number (B), and Prandtl's number, impact temperature distribution. These insights hold significance for numerous applications, including thermal management systems in industrial processes, geothermal energy extraction, and designing cooling systems for electronics. The comprehensive numerical computations encompass all feasible aspect ratio (M) and Bingham number (B) values, providing valuable insights into optimizing heat transfer performance. Additionally, this study visually demonstrates the temperature distribution across the radial direction (R), aiding in the interpretation and application of the results in real-world scenarios. The following can be drawn from this investigation.

1. From the annulus's still internal partition to its turning external partition, the temperature rises.
2. The temperature is seen to rise as the Bingham numeral B is increased.
3. It is exposed that the temperature rises as aspect ratio M grows.
4. The temperature also rises as axial position Z increases.
5. From the inner to the outer wall of the annulus there is a significant upsurge in the tangential velocity.
6. Increasing the aspect ratio (M) results in a corresponding increase in axial velocity across all examined variations of Bingham numbers (B).
7. This study reveals that radial velocity is dependent on the axial coordinate.
8. From the inner to the outer wall there is a significant upsurge in the pressure, while it shows a minimal variation near the outer wall.
9. It seems that there is not much of an impact of outer wall rotation on these flow parameters.

Overall, this paper contributes to the understanding of heat transfer phenomena in concentric annuli with rotating outer walls, particularly when dealing with Bingham fluids. The analysis of various parameters provides valuable insights into the complex interplay between fluid dynamics and heat transfer in such systems.

REFERENCES

[1] Coney, J.E.R., El-Saharawi, M.A.I. “A contribution to the numerical solution of developing laminar flow in the entrance region of concentric annuli with rotating inner walls” Journal of Fluids Engine- ring, 1974; 96(4): 333-340, DOI: 10.1115/1.3447166

[2] Mishra, I.M., Kumar, S.,Mishra, P. “Entrance region flow of Bingham plastic fluids in concentric annulus.: Indian Journal of Technology, 1985; 23: 81-87.

[3] Batra, R. L., Das, B. “Flow of Casson Fluid between two Rotating Cylinders.” Fluid Dynamic Research, 1992; 9: 133-141, DOI: 10.1016/169-5983(92090063-3

[4] Maia, M.C.A., Gasparetto, C.A, “A numerical solution for entrance region of non-Newtonian flow in annuli, “Brazilian Journal of chemical Engineering, 2020; 2003: 201-211, DOI:10. s1590/0104-6632003000200014

[5] Sayed-Ahmed, M.E., Sharaf-El-Din,H. “ Entrance region flow of a power-law fluid in concentric annuli with rotating innerwall.” International Communications in Heat and Mass Transfer, 2006; 33(5): 654-665, DOI: 10.1016/j.icheatmasstransfer.2006.01.004

[6] Bird, R.D., Dai, G.C. Yarusso, B, J. “The rheology and flow of Visco plastic materials.” Reviews in chemical Engineering, 1982; 1: 1-70.

[7] Kandasamy, A. “Entrance region flow heat transfer in concentric annuli for Bingham fluid.” In Third Asian-Pasific conference on Computational Mechanics, Seoul, Korea, sept. 1996; 16-18: 1697-1702.

[8] Galanis,N. Rashidi, M.M. “ Entropy generation in Non-Newtonian fluids due to heat and mass transfer in the entrance region of ducts.” Heat and mass Transfer, 2012; 48(9): 1647-1662.

[9] Round, G.F,Yu.,S. “ Entrance laminar flows of viscoplastic fluids in concentric annuli.” The Canadian journal of chemical engineering, 1993; 71(4):642-645, DOI:10.1002/cjce.5450710417

[10] Nadimiti S. R, Kandasamy, A. “Entrance region flow of Heat transfer in concentric annuli with Rotating inner wall for Bingham Fluid” Periodica polytechnic Mechanical Engineering, 2016; 60(3):167-179, DOI:10.3311/ppme.8970

[11] A. A. Zadorozhnyi, Architectural construction using technologies based on knowledge about the flow of Bingham plastic fluids in various pipelines, IOP Conference Series: Materials Science and Engineering, 2020; 907: 012028, DOI: 10.1088/1757-899X/907/1/012028

[12] Mullai Venthan, and I. Jayakaran Amalraj, Numerical Investigation of Bingham Fluid Flow in the Entrance Region of Rotating Annuli, Trends in Mechanical and Biomedical Design, 2021; 499-518, https://doi.org/10.1007/978-981-15-4488-0_42

[13] V K Chithrakumar, G Venugopal and M R Rajkumar**,** Thermal behavior of heated stationary inner cylinder of a concentric vertical annulus formed with rotating outer cylinder, IOP Conference Series: Materials Science and Engineering, 2021; 1114: 012050, DOI: 10.1088/1757-899X/1114/1/012050

[14] Arain, M.B., Zeeshan, A., Bhatti, M.M. et al. Description of non-Newtonian bioconvective Sutterby fluid conveying tiny particles on a circular rotating disk subject to induced magnetic field. J. Cent. South Univ. 2023; 30: 2599-2615, https://doi.org/10.1007/s11771-023-5398-1

[15] Bhatti, M. M., Bég, O. A., & Kuharat, S. Electro magneto hydrodynamic (EMHD) convective transport of a reactive dissipative Carreau fluid with thermal ignition in a non-Darcian vertical duct. Numerical Heat Transfer, Part A: Applications, 2023; 1-31, https://doi.org/10.1080/10407782.2023.2284333

[16] Pratik Anhor and Mohammad Atif, Effect of outer-cylinder rotation on the radially heated Tylor-Couette flow, Physics of Fluids, 2023; 35(9): 094108, https://doi.org/10.1063/5.0160816

[17] Babu, B. Hari, Rao, P. Srinivasa, Varma, S. V. K. Heat and mass transfer on Unsteady MHD convective flow of Casson hybrid nanofluid over a permeable media with ramped wall temperature. *Journal of Nanofluids* 11(4), 552-562, 2022. https://doi.org/10.1166/jon.2022.1864

[18] Hari Babu B. Heat and mass transfer on unsteady MHD Casson fluid flow past an infinite vertical porous plate with chemical reaction. *Proceedings of the Institution of Mechanical Engineers, Part E: Journal of Process Mechanical Engineering*. 237(6):2278-2289, 2023; doi:10.1177/09544089221133966

[19] Babu BH, Rao PS, Reddy MG, Varma SVK. Numerical modelling of activation energy and hydromagnetic non-Newtonian fluid particle deposition flow in a rotating disc. *Proceedings of the Institution of Mechanical Engineers, Part E: Journal of Process Mechanical Engineering*. 2023;237(2):108-117. doi:10.1177/09544089211045907

[20] B. Hari Babu, P. Srinivasa Rao, S. V. K. Varma. Hall and ion-slip effects on MHD free convection flow of rotating Jeffrey fluid over an infinite vertical porous surface, *Heat Transfer*, 2020, https://doi.org/10.1002/htj.21954

[21] Hari Babu, B., Rao, P. S., Reddy, M. G., Varma, S. V. K. Non-linear radiation and dissipative impacts on non-Newtonian hydromagnetic Falkner-Skan fluid through a wedge. *Waves in Random and Complex Media*, 1–16, (2022). https://doi.org/10.1080/17455030.2022.2121448